

Supplement of Atmos. Meas. Tech., 12, 5431–5441, 2019
<https://doi.org/10.5194/amt-12-5431-2019-supplement>
© Author(s) 2019. This work is distributed under
the Creative Commons Attribution 4.0 License.



Supplement of

A low-cost monitor for simultaneous measurement of fine particulate matter and aerosol optical depth – Part 1: Specifications and testing

Eric A. Wendt et al.

Correspondence to: John Volckens (john.volckens@colostate.edu)

The copyright of individual parts of the supplement might differ from the CC BY 4.0 License.

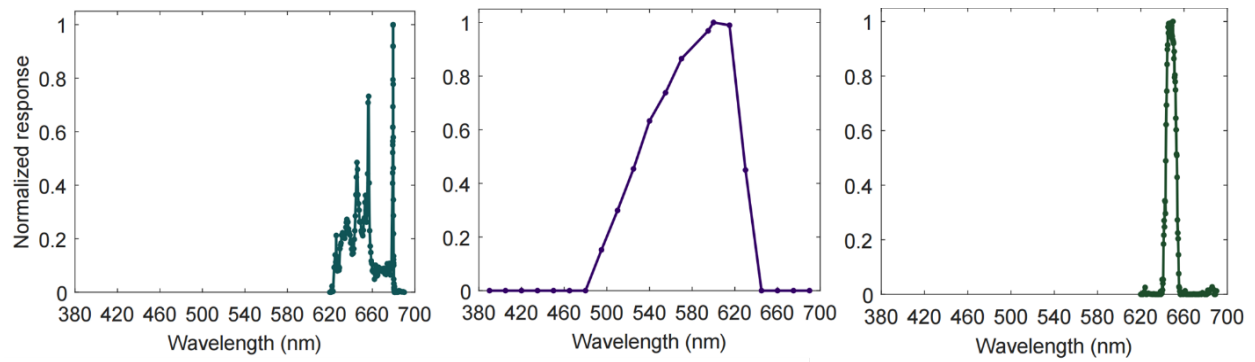


Figure S1: Spectral response curves for (a) 680 nm VCSEL, (b) 620 nm LED and (c) 650 nm filtered photodiode. The vertical axis gives the detector response normalized with respect to light source power and maximum detector signal output.

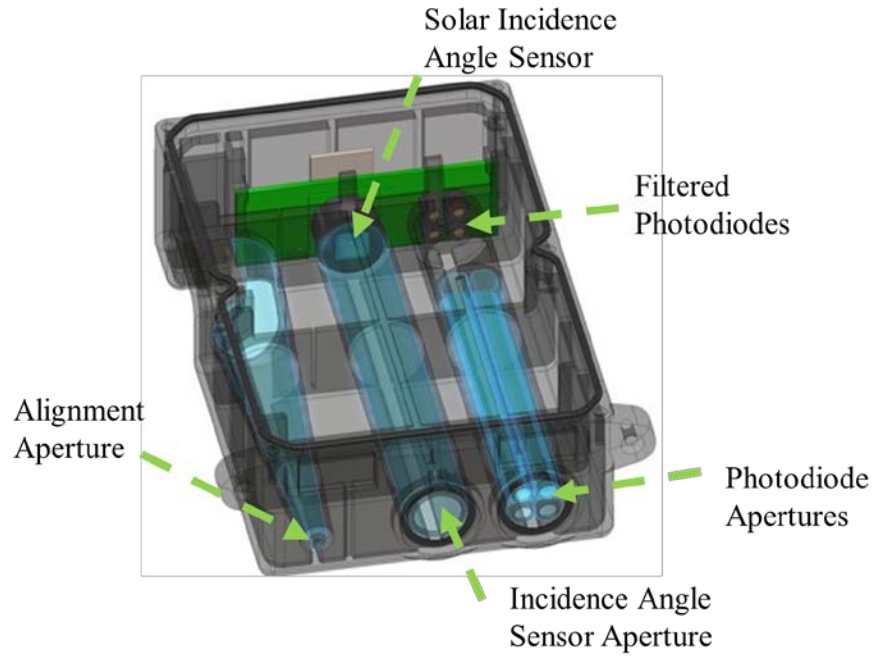


Figure S2: CAD rendering of AMOD AOD measurement system including the light apertures and electronic hardware components. Light blue shading indicates a hollow region for light transmission; black and green shading indicate the housing and AOD circuit board, respectively.

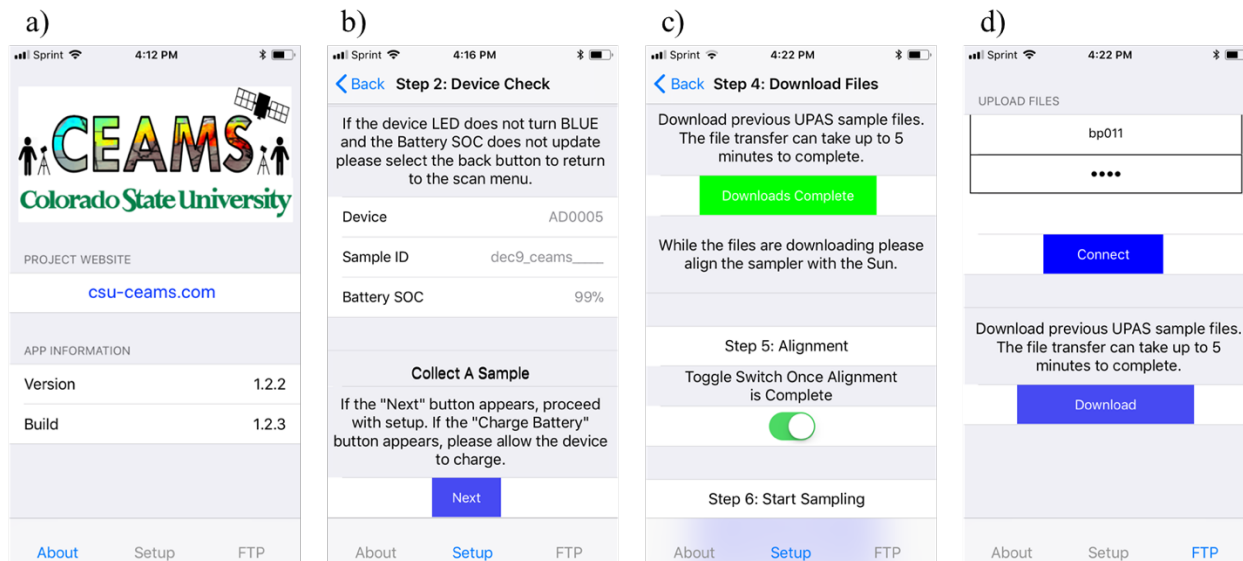


Figure S3: Smartphone application screenshots summarizing the key steps in the AMOD setup process: (a) Information and website link; (b) quality assurance check; (c) data download and alignment check; (d) file upload using standard file transfer protocol.



Figure S4: Two AMOD samplers mounted with an FEM gravimetric filter sample and next to the GRIMM FEM monitor for a co-location test.

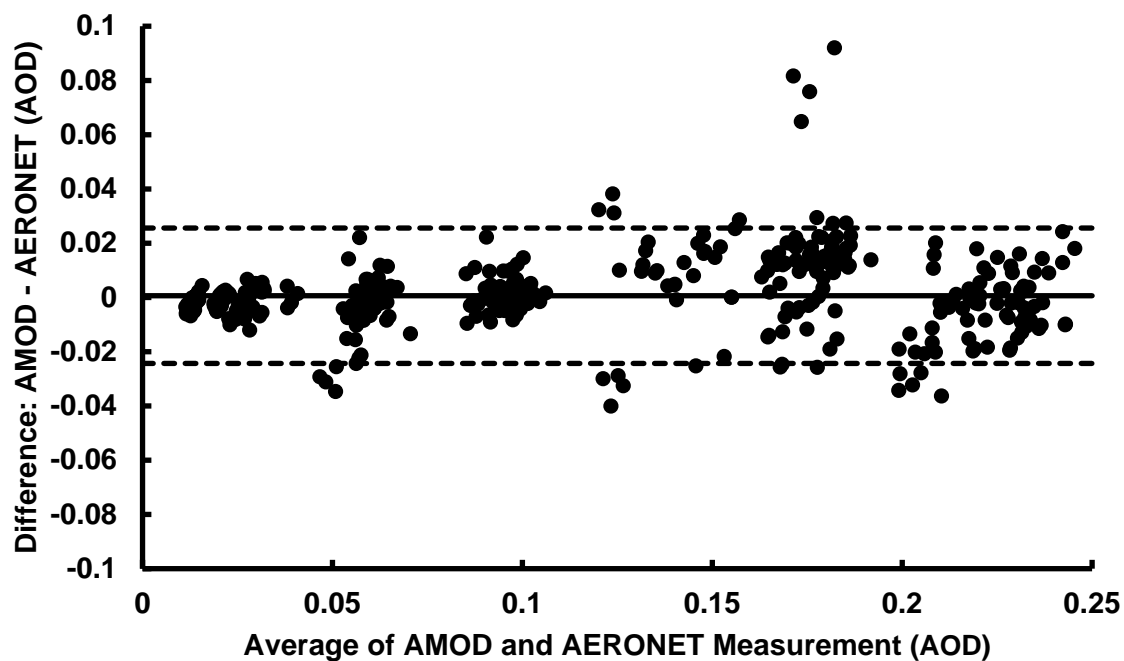


Figure S5: Bland-Altman plot for AOD measurements taken by AERONET and AMOD monitors. Points represent paired AMOD and AERONET measurements with the average of the measurement pair on the x-axis and the difference on the y-axis. This plot includes all measurements ($n = 520$) taken across all wavelengths as part of the 2017 co-location campaign. The top and bottom dashed lines represent the upper and lower limits of agreement, respectively, evaluated at 95% confidence. The solid line in between the limits of agreement is the mean difference between the two measurement techniques.

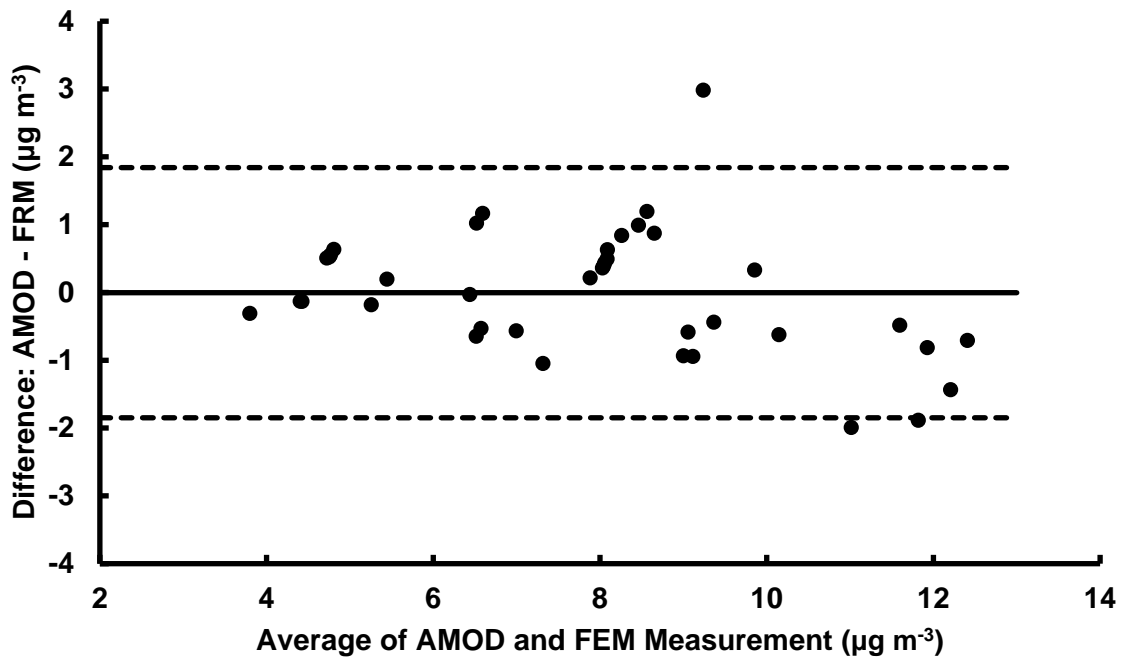


Figure S6: Bland-Altman plot for PM_{2.5} mass concentrations measured using FEM and AMOD filter samples. Points represent paired AMOD and FEM measurements with the average of the measurement pair on the x-axis and the difference on the y-axis. The top and bottom dashed lines represent the upper and lower limits of agreement, respectively, evaluated at 95% confidence. The solid line in between the limits of agreement is the mean difference between the two measurement techniques.

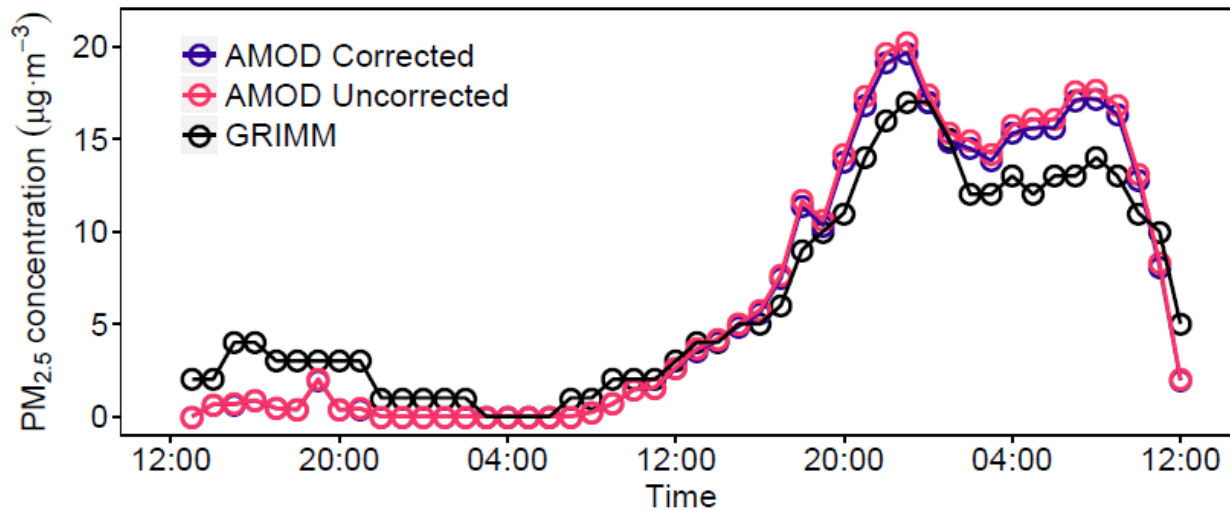


Figure S7: Representative 48-hr time series comparison plot between the AMOD light-scattering sensor (corrected and uncorrected) and an FEM GRIMM light-scattering sensor.

Table S1: AMOD Cost of Goods and Assembly Summary

Component	Manufacturer	Part Number	Cost
Printed Circuit Boards	NOVA Engineering	Custom Parts	\$475
440 nm Filtered Photodiode	Intor	Unavailable	\$28
520 nm Filtered Photodiode	Intor	Unavailable	\$26
680 nm Filtered Photodiode	Intor	Unavailable	\$26
870 nm Filtered Photodiode	Intor	Unavailable	\$28
Light-Scattering PM _{2.5} Sensor	Plantower	PMS5003	\$15
Solar Alignment Sensor	Solar MEMS	NANO-ISS5	\$45
AMOD Housing	Xometry	Custom Part	\$130
Cyclone and Inlet	Synergy Core	Custom Part	\$74
3.5 W Solar Panel	Voltaic	Unavailable	\$35
Battery Pack	Battery Space	CU-JAS380	\$94
Misc. Housing Components	N/A	N/A	\$44
Assembly Labor	N/A	N/A	\$50
Total Costs			\$1075